NDE Applications of Air-Coupled Ultrasonic Transducers

W.A. Grandia[1] and C.M. Fortunko[2]

[1] Quality Material Inspection Inc., Costa Mesa, CA 92627
[2] National Institute of Standards and Technology, Boulder, CO 80303

Abstract -- In recent years, several new NDE applications of air-coupled, as opposed to liquid-coupled, ultrasonics have been seriously pursued. The applications range from through-transmission testing of aerospace laminates and various honeycomb or foam filled materials, and solar cells, to pulse-echo flaw detection in plastic electronic packaging materials and in-line inspection of large-diameter gas pipelines. Most of the new applications have been made possible by major advances in component technologies: transducers, pre-amplifiers, pulsers, signal-conditioning, and impedance matching and noise-matching circuits. In this paper, we describe the transducer types and circuit topologies that are especially suitable for applications in the 20 kHz to 20 MHz frequency region. We also address the important key differences between air-coupled and liquid-coupled inspection configurations. In particular, we focus on the practical advantages and limitations that arise from the fact that gases and liquids exhibit substantially different specific densities and sound speeds.

I. INTRODUCTION

Ultrasonic "water-immersion" and "water-squirt" scanning systems are widely used in nondestructive testing[1]. Water is attractive as a coupling medium, because it is universally available, exhibits insignificant absorption at low MHz frequencies, and generally does not affect the physical, chemical and mechanical properties of most industrially-important materials. However, water is not compatible with some industrial processes and may cause permanent damage to paper, open-cell foams, many reinforced plastics and wood products, propellants and explosives, art objects, certain electronic-packaging materials, and many materials intended for use by the aerospace industry. Also, the use of water appears to reduce the surface-flaw detection probabilities in polymer-matrix and internal flaws in porous materials. The specific acoustic impedance of such materials is of the same order of magnitude as that of water, lying in the range 1-10 Mrayls. Consequently, there is a genuine need for ultrasonic flaw-detection systems that do not use water and other liquids as the coupling medium[2]. In the past three decades, relatively large resources have been dedicated to the study and development of various non-contact ultrasonic inspection systems[3], principally those that rely on the use electromagnetic-acoustic transducers (EMATs)[4,5,6,7] or lasers[8,9,10] for generation and reception of the ultrasonic probing signals. Combined EMAT/laser[11,12,13] air-transducer/laser[14] systems have also been investigated. During the same period of time, relatively modest resources have been appropriated for exploration and development of ultrasonic inspection systems that rely on air, or another gas, as the coupling medium. In spite of this, there have been significant advances in the state of the art of air-coupled inspection systems, resulting in practical industrial applications of the technology[15]. There is now also a greater interest in the academic community, which recognizes the inherent advantages of using non-contact transducers in materials characterization studies[16,17,18,19] and flaw-detection[20,21,22,23] .

Air-coupled ultrasonic inspection can be considered as a non-contact or minimally-invasive method, because the coupling medium (air or another gas) is part of the natural environment and therefore no additional physical contact is required. The use of air coupling is particularly attractive, because it results in ultrasonic probing signals whose temporal and spatial characteristics are similar to those generated using water coupling. This makes air-coupled systems particularly appropriate in applications that are not well suited for the use of EMAT or laser-based systems. In particular, such applications include the nondestructive testing and characterization of many polymer-based aerospace composite materials. Most of the elastic-wave types generated and detected by lasers can also be generated and detected using air-coupled systems. On the other hand, air-coupled systems cannot be used to generate and detect certain elastic-wave types (e.g. torsional waves) that can be easily generated and detected by EMATs[24].

II. BRIEF HISTORICAL PERSPECTIVE

Air-coupled ultrasonic NDE has been enabled by the availability of transducers. The transducers, which are best suited for use in air-coupled ultrasonic NDE systems, have been initially developed for other applications: process control, gas-flow measurement, proximity sensing and distance gauging, and the like. In such applications, it is often

0-7803-2940-6/95/$4.00

essential to operate in the frequency region that extends from 25 kHz to 2.5 MHz. This frequency region overlaps that of practical interest in ultrasonic NDE.

In a recent publication, V. Magori reviewed the characteristics of various practical air-coupled transducers that are used in propagation-path sensors, including gas-flow meters, and distance sensors in air-sonar applications[25,26]. However, for historical reasons, it is also important to include references to the pioneering work of L.C. Lynnworth[27,28], F. Massa[29,30], W. Kuhl and co-workers[31], W.W. Wright[32,33], who developed the solid-dielectric microphone, technical-staff members at the Polaroid Corporation[34], and B.T. Khuri-Yakub[35]. The availability of such transducers has also enabled the work leading to the determination of universal gas constant R, the sound speeds, and other properties of gases[36,37]. A brief review of the physics of such transducers is given by M. Trusler[38].

The propagation characteristics of ultrasound in the air and other gases have also received considerable attention. For example, Hickling and Marin describe phenomena that affect the use of 1MHz sound signals in gauging and proximity sensing applications[39]. The physical phenomena of sound absorption in the atmosphere in the audio region are reviewed in great detail by H.E. Bass et al.[40], while the effects of turbulence on apparent attenuation are addressed by E.H. Brown and S.F. Clifford[41]. In the ultrasonic frequency region, above 20 kHz and below 1 MHz, sound absorption information, as a function of frequency, relative humidity, and pressure, can be obtained by using published expressions[42,43]. The use of the published expressions is probably justified up to 10 MHz, and even higher, frequencies[44].

The potential advantages and limitations of using air-coupling in nondestructive material inspections have been recognized for a long time[45]. In particular, air coupling was found desirable in applications involving the inspection of materials that could not be immersed in water or that would be damaged by physical contact with an ultrasonic transducer. Such materials include propellants[46], certain wood and paper products[47,48], foams, art objects[49], and many advanced composite materials used by the aerospace industry[50]. Measurement of tension in a paper web has also been reported[51].

Initially, practical applications were confined to the 25-250 kHz frequency region[52]. Later, improvements in piezoelectric transducer-design technologies and electronics have made it feasible to operate in the 0.5-1.0 MHz frequency region[53,54]. Recently, the possibility of using gas-coupled systems to carry out in-line inspections of natural-gas pipelines has been investigated[55]. Also, the feasibility of a gas-coupled acoustic microscope, operating in a pulse-echo, c-scan mode, using argon at elevated pressure (30 atm and higher), has been demonstrated[56]. Such devices must operate at frequencies of 5 MHz, and higher, to compete with water-coupled systems. Previously, a gas-coupled system, operating at 45 MHz and 30 atm, was reported[57]. However, this system was intended primarily to study the topographic features of surfaces.

III. FUNDAMENTAL OBSTACLES TO AIR-COUPLED NDE

It is widely believed that atmospheric absorption is the major obstacle to the use of air-coupled ultrasonic inspection systems. This is not so. It can be readily shown that, in the frequency region of interest, the limitations are due to the very large specific acoustic impedance differences between typical solids and gases. In a system that uses air-coupled transducers for both generation and detection, the received signal amplitude is principally determined by the transmission losses at the four air/solid interfaces, as shown in Fig. 1. Additional, but significantly smaller, losses can also be expected due to diffraction, loss of phase-front coherence, and finite-amplitude saturation effects, which are sometimes experienced at very high drive levels.

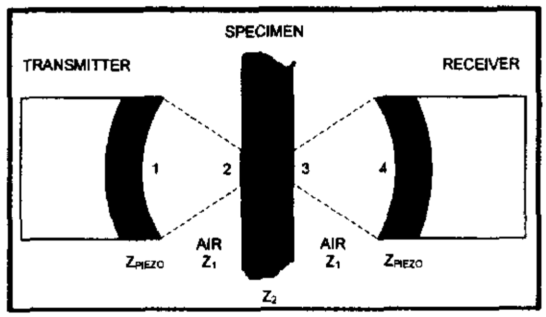

Fig. 1 Air to solid interfaces 1, 2, 3, 4.

The signal-to-noise performance of an air-coupled system can be estimated using:

$$S/N = 10\log\left(\frac{Pa}{4kT\Delta f} \cdot \frac{D}{NF*CL*AL*AB*DL*EL}\right) \quad (1)$$

where Pa is the available transmitter power, k is the Boltzmann's constant, T is the absolute temperature in °Kelvin, and Δf is the effective bandwidth of the receiver electronics, and NF is a "noise factor". In practice, NF ranges from 1 to 10 and depends on the effectiveness of the procedure used to increase the electrical input resistance of the receiver transducer to the resistance level corresponding to the equivalent noise resistance of the preamplifier. NF can be reduced by using an impedance-matching transformer, or by taking advantage of the self-resonance of the transducer, or both. D is the bulk transmission $D=T_1*T_2$, where T_1 and T_2 are the interface transmission coefficients. CL further accounts for the two-way transducer conversion loss; AL for sound absorption in the air; AB for the absorption in the specimen; DL for diffraction losses; and EL for "excess" propagation losses due to finite-amplitude saturation effects and partial loss of phase-front coherence due to specimen-surface topography and internal elastic inhomogeneity and air turbulence effects. In most applications, diffraction and "excess" propagation losses can be neglected (DL=EL=1).

The available transmitter power is given by:

$$Pa = V^2/4R \qquad (2)$$

where V is the peak-to-peak voltage and R is the output-loading resistance of the pulser or amplifier. Currently, typical voltages are in the 400-volt range while output-loading resistance as low as 4 ohms is attainable. Consequently, available powers in the range of 10 kW can be achieved using commercially available power transistors. Assuming (very optimistically) a receiver-electronics bandwidth of 100 kHz and NF = 1, the electrical-noise power at the receiver input is approximately 1.66 fW. Consequently, the available signal-to-noise is nearly 188 dB. Of course, this level of performance can be achieved only by using very efficient electrical impedance and noise matching networks at the transmitter and preamplifier, respectively.

Assuming that the specimen is thick compared to the wavelength and nonresonant, the transmission term D in Eq. 1 can be estimated from:

$$D = 4\, Z_1 Z_2 \,/\, (Z_2 + Z_1)^2 \qquad (3)$$

where Z_1 is the specific acoustic impedance of air and Z_2 is the specific acoustic impedance of the specimen. In practice we read amplitude ratios A_1/A_2, which are given in decibel readings according to $dB = 20\log(A_1/A_2)$, as are all the following estimates. Since the specific acoustic impedance of air is 0.0004 Mrayl and that of typical solids is in the range 1 to 50 Mrayls, D can be expected to be in the range 56 to 90 dB.

Equation 3 can also be used to estimate the two-way transducer conversion loss term, CL. Since the specific acoustic impedance of a high-power piezoelectric material, such as PZT-5A, is approximately 35 Mrayl, the transducer conversion losses can be as high as 87 dB.

Finally, the air-absorption losses, AL, can be estimated using formulae published by Bass et al.[40,42,43]. Following the American National Standard[58], Figure 2 shows the behavior of the absorption coefficient for air at atmospheric pressure in the frequency region. 10 Hz to 1 MHz.

It is seen that in the practically important frequency region, 100 kHz to 1 MHz, the absorption coefficient is in the range - range of 10 to 100 dB/m. Thus, at a typical working distance of 50 mm, the two-way absorption losses, AL, should not be in excess of 10 dB at 1 MHz, atmospheric pressure, and 300° K. Consequently, sound absorption in air is not a serious issue in practice.

From the above, it is evident that, at 1 MHz, the transmission losses as contributed by D, CL, and AL, can range from 153 dB, for foam-type materials (1 Mrayl), to 189 dB, for materials such as steel (48 Mrayls). At best, a signal-to-noise factor of 33 dB can be achieved in the case of a very light material, such as foam or balsa wood. However, such materials also exhibit high attenuation. On the other hand, in the case of steel, a signal-to-noise deficit of 1 dB can be expected. Of course, signal-averaging procedures can, in principle, be employed to increase the signal-to-noise performance of an air-coupled inspection system. However, we do not consider this a viable option, because of the economic realities that ultimately determine the commercial success of a nondestructive testing procedure. We believe, strongly, that practical ultrasonic systems must be capable of operating in real time.

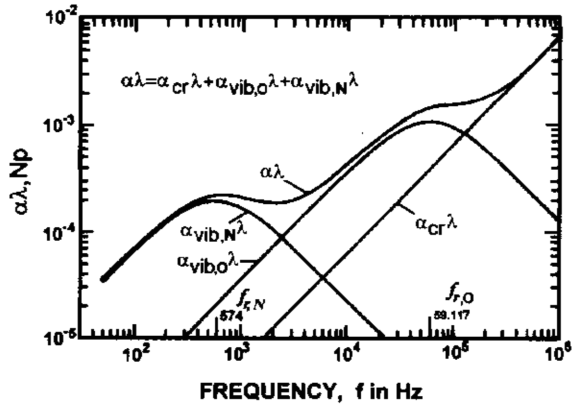

Fig.2. Absorption per unit wavelength for acoustic waves in air at 293.15 K (20 °C), 101.325 kPa and 70% relative humidity (after ANSI). Here, $f_{r,N}$ is the vibrational relaxation frequency for nitrogen; $f_{r,O}$ is the vibrational relaxation frequency for oxygen (copyright Acoustic Society of America)

Obviously, useful signal-to-noise performance cannot be achieved without decreasing the conversion losses, CL, of the transducers or, by some means, enhancing the transmission D associated with the specimen material. It goes without saying that proper electrical-design and construction rules must also be followed to realize very efficient electrical impedance and noise matching networks at the transmitter and receiver preamplifier. In this paper, we show how this can be done by improving the efficiency of the transducers by better matching of the transducer mechanical impedance to the net-reaction impedance of the air or another coupling gas, taking advantage of the physical features of the specimen material, and increasing the ambient pressure of the air or gas.

IV. Practical Transducers for Air-Coupled Ultrasonic NDE

Transducers for the generation and reception of sound are without doubt the most critical components of an air-coupled ultrasonic NDE system. Six types of electro-acoustic air transducer types are potentially of interest: electrostatic, variable reluctance, moving coil, piezoelectric, electrostrictive, and magnetostrictive. Figure 3 summarizes the frequency regions that can be covered using different practical mechanizations.

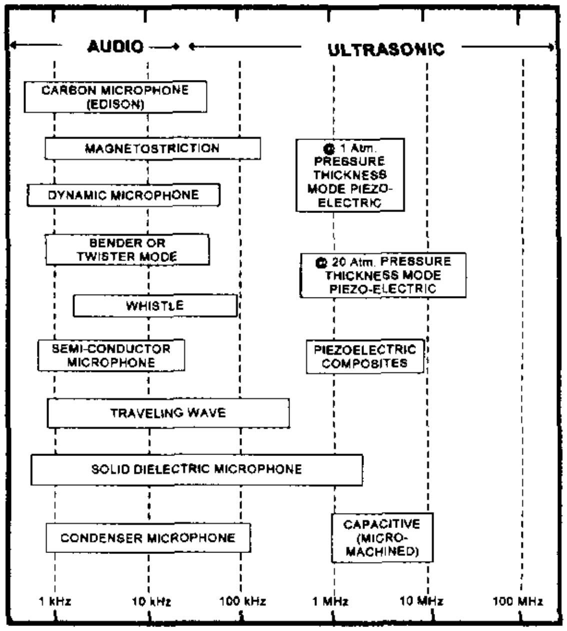

Fig. 3. Frequency range of various air transducers.

It is interesting to note that the piezoelectric and electrostatic transducers are represented by several implementations. For example, the class of electrostatic transducers includes the condenser microphone, the solid-dielectric microphone, and the new wide-band, capacitive transducer, which is made using silicon-micro-machining techniques. There are also several different piezoelectric transducers, including the low-frequency "bender" types as well as the thickness-mode, conventional and composite piezoelectrics.

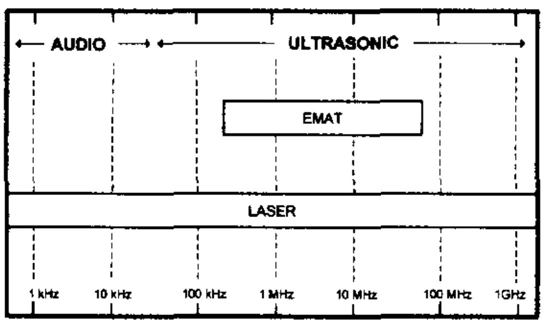

Fig. 4. Frequency range of complementary non-contact transducers

For completeness, Figure 3 also includes a carbon microphone and whistle; although use of these devices for practical NDE applications has not been reported in the literature, to the authors' knowledge, at the present time.. Figure 4 specifies the frequency regions of other transduction methods, which do not employ the air as a coupling medium, such as EMAT and laser-based transducers, and which may be used in practical applications in conjunction with air transducers. To address current commercial applications, we rely mainly on the thickness-mode, piezoelectric transducer types. We use both focused and flat transducers (Fig 5), depending on application. On occasion, particularly when inspecting thick inhomogenous materials, we also use a combination of flat and focused transducers. The through-transmission and pitch-catch configurations are widely used for a variety of applications. At the present time, the pulse-echo configurations cannot be realized at atmospheric pressures. However, it has been successfully demonstrated at elevated pressures, typically above 30 atmospheres. Potentially, this configuration may have important practical applications, including in-line inspection of natural-gas pipelines and gas-coupled, acoustic microscopy of electronic-packaging materials.

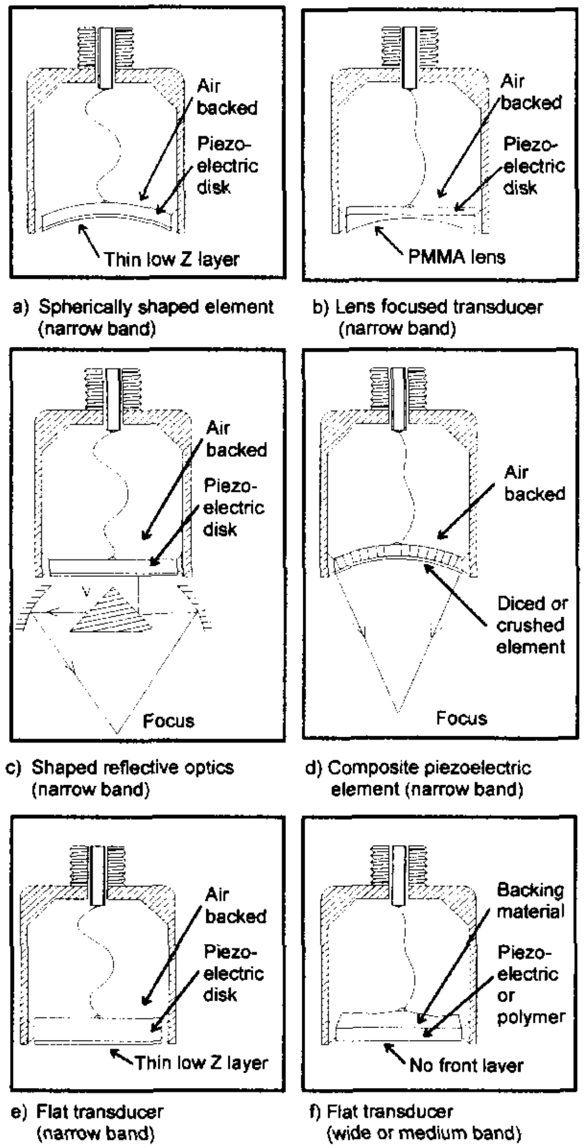

Fig. 5. Thickness-mode piezoelectric air transducers

The operation of a piezoelectric transducer designed for operation in air is best explained using the flat transducer as an example. Typically, such transducers are constructed using a circular disk of an efficient piezoelectric ceramic material, such as PZT-5A. Frequently, we also employ a thin layer of a porous material with low specific acoustic impedance to improve the generation and reception efficiencies. However, we do not use a backing layer. We do so to take advantage of the high mechanical-quality factor Q of the piezoelectric disk. As a consequence, such transducers can be operated in the resonant-mode, resulting in much higher sensitivities. Typically, mechanical Q's as high as 10 can be achieved at 500 kHz using a 25-mm-diameter PZT-5A disk. The construction of a typical flat air transducer is shown in Figs. 5e and 5f.

The transducer shown in Fig. 5a is best suited for operation in the tone-burst mode, which is frequently used in through-transmission and pitch-catch testing of aerospace laminates. In this case, the center frequency of the driving electrical signal is chosen to correspond exactly to the thickness-mode resonance of the transducer. As a consequence, the transmit and receive sensitivities can be increased by as much as 20 dB. However, such transducers are necessarily narrow-band and can be operated only at one frequency. On the other hand, the signal-to-noise performance of systems using the resonant piezoelectric transducers frequently exceeds 40 dB. Such systems can be operated in real time, without the need for signal averaging. Also, such systems can be aligned by relatively inexperienced operators, a distinct benefit in the commercial-inspection environment.

In the past, we have also successfully employed flat, broad-band piezoelectric transducers. The construction of this type of transducer is shown in Fig. 5f. In contrast to the resonant transducer, shown in Fig. 5e, the broadband transducer does not utilize a front-face layer for improving the impedance match between the gas and piezoelectric material. The use of an impedance-matching layer would significantly reduce the bandwidth of the transducer. Also, the transducer in Fig. 5f uses an efficient backing material that prevents multiple reverberations within the piezoelectric layer. In the past, we have successfully used both piezoelectric ceramic and polymer materials to construct such transducers for pulse-echo operation at elevated pressures. It is important to add that pulse-echo operation cannot currently be achieved at atmospheric pressures using such transducers.

At the present time, spherically-focused piezoelectric transducers appear to be more useful than flat transducers. Several methods of constructing such transducers are depicted in Figs. 5a - d. The simplest method, shown in Fig. 5a, uses a spherically-shaped piezoelectric ceramic disk. Such disks are also used to construct conventional piezoelectric transducers for water-immersion C-scan systems. Figure 5b shows a transducer that uses a flat piezoelectric disk and a refractive lens made of a light material, such as polymethylmethacrylate (PMMA). In Fig. 5c, the same goal is achieved by using suitably-shaped reflective optics[59]. Finally, Fig. 5d shows a spherically-focused transducer using a composite piezoelectric material. Spherically-focused transducers are of great interest, because they provide excellent signal-to-noise performance in the 100 kHz - 1 MHz frequency region, particularly when inspecting aerospace laminates with complicated internal geometries. When inspecting thin aerospace laminates, we frequently operate at signal-to-noise ratios in excess of 40 dB at 400 kHz.

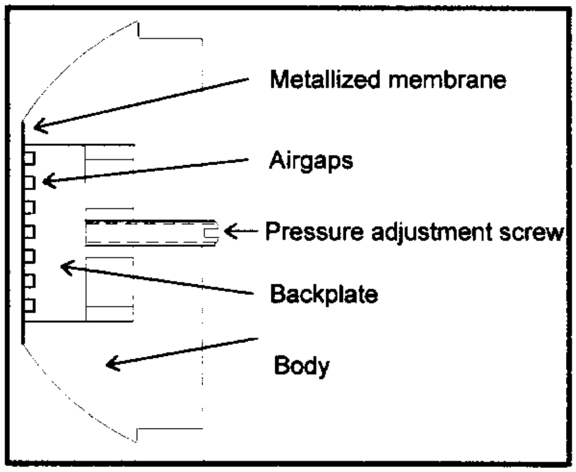

Fig. 6a. Solid dielectric condenser microphone/transmitter (After W. Kuhl et al.[31])

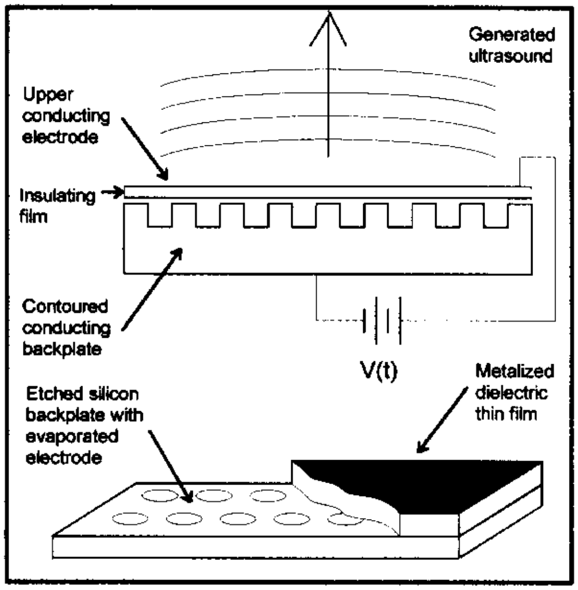

Fig. 6b. Schematic diagram of a capacitance transducer for generation and detection of ultrasound in air (After D.W. Schindel et al.[68])

Piezoelectric transducer technology is now very mature. At the present time, systems using such transducers already operate at the physical limits of the piezoelectric materials, assuming the dielectric breakdown to be the dominant damage mechanism, and semiconductor switching devices. It is interesting to note that, assuming a 2 V/μm dielectric breakdown strength, a 25-mm-diameter PZT-5A disk can handle approximately 15 kW of peak electrical power. In practice, such power densities are not achievable since strains larger than 10^{-4} (ratio of displacement to total thickness), corresponding to 0.1 μm front-surface displacements at 2 MHz, cannot be sustained for extended periods of time[60]. At the present time, 10 kW is the maximum electrical power that can be delivered by practical ultrasonic pulsers or gated amplifiers. Because of the very inefficient acoustic-impedance matching at the front face of the transducer, most of the available transmitter power is uselessly converted to heat in the transducer or returned to the transmitter.

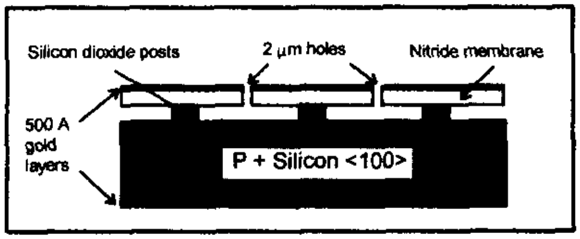

Fig. 6c. Schematic diagram of a surface micromachined electrostatic ultrasonic air transducer (After M.I. Haller and B.T. Khuri-Yakub[61])

Transduction efficiency can, in principle, be improved by using an impedance-matching layer, or reducing the specific acoustic impedance of the transducer material. The former approach can be only partially successful, because practical impedance matching materials (cork, balsa wood, silicone rubber, etc.) exhibit very low mechanical Q's[61]. Using the piezoelectric-composite[62] approach, as shown in Fig. 5d, results in a transducer with significantly reduced capacitance. In fact, this effect appears to directly offset any benefit of using a material with reduced acoustic impedance.

Because acoustic-impedance matching materials having a characteristic impedance of less than 1 Mrayl are currently inconsistent, there is now considerable interest in developing other transducer types, principally those using the electrostatic transduction mechanism. Therefore, it is of interest to review the state-of-the-art and practical limits of this transducer technology. Three different transducer types, each employing the electrostatic mechanism, are shown in Fig. 6a-c.

At low frequencies, below 100 kHz, condenser microphones, as shown in Fig. 6a, can be used to generate and receive ultrasonic signals in air[63,64]. In the condenser microphone, the restoring force is provided by the tension in the membrane, which is typically made of high-strength steel. Unfortunately, conventional transducers of the condenser type are not suitable for our applications, because the resonant frequency of the membrane is physically limited by material considerations.

Figure 6b shows another type of an electrostatic transducer, the solid-dielectric microphone, which can operate at frequencies well above 100 kHz. This device does not use applied tensile forces to restore the position of the membrane, but achieves a much better match to air than the various piezoelectric, thickness-mode transducers. The restoring forces are principally due to the presence of air pockets between the membrane and back plate[65,66]. Recently, there has been a resurgence of interest in this type of transducer, principally as a result of advances in micro-machining technologies[67,68]. Potentially, the new construction techniques can result in better-designed transducers, with performance characteristics that can be predicted.

The two-way insertion losses of the solid-dielectric transducers can also be estimated using Eq. 3, but by assuming that the specific acoustic impedance of the membrane is given by,

$$Z1 = j2\pi f\rho t \quad (4)$$

where j is the square root of -1, f is the frequency, ρ is the specific density, and t is the thickness of the membrane material. (It is interesting to note that the product ρt is simply the mass per unit area of the membrane.)

Assuming that the membrane is made of polyethylene terephthalete (PET; Mylar^{TM}), 10 μm thick, the two-way insertion loss is approximately 67 dB at 500 kHz, a 20-dB improvement relative to a piezoelectric (PZT-5A), thickness-mode transducer. However, we have found the commercially available transducers to be less sensitive than the state-of-the-art piezoelectric, thickness-mode transducers.

Figure 6c shows a new micromachined capacitive air transducer that uses a much thinner membrane (0.5 μm vs. 2.5-10 μm) than the current-generation solid-dielectric microphones[69]. The new transducer appears to embody the most desirable features of condenser and solid-dielectric microphones. In particular, it uses the residual stresses in the membrane to provide the restoring forces. Consequently, it can achieve a sensitivity and dynamic range significantly higher than that of the solid-dielectric microphone. In the transmission mode, front-surface displacements as high as 0.3 μm have been reportedly achieved at 2 MHz. The front-surface displacements are higher than those now obtainable using PZT-5A, thickness-mode transducers. Fractional bandwidths reportedly range from 5 to 20%. Also, the new transducers are also more efficient and, therefore, do not require the high-cost, high-power pulsing systems needed to drive the piezoelectric, thickness-mode transducers. Furthermore, since the air gaps behind the membrane have a depth of only 1 μm or so, the new transducers exhibit large input capacitances, resulting in efficient noise matching to the receiver preamplifier. We hope that the new transducers will soon become available to the designers of ultrasonic NDE systems since their impact on cost and performance of such systems may be very significant.

V. A PRACTICAL AIR-COUPLED ULTRASONIC INSPECTION SYSTEM FOR AEROSPACE MATERIALS

Figure 7 shows an air-coupled ultrasonic flaw detector which has been designed for a variety of NDE applications, primarily in the aerospace industry. A practical C-scan inspection configuration is shown in Fig. 8, and a functional block diagram of this system is shown in Fig. 9.

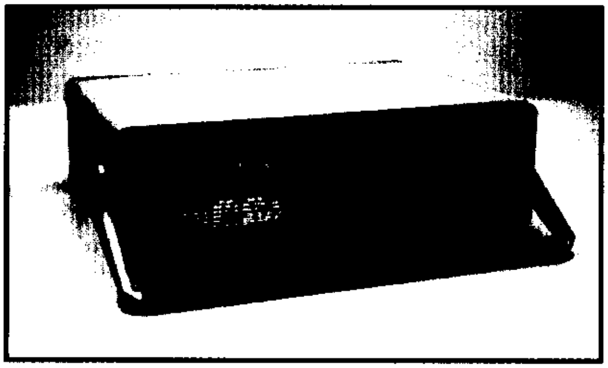

Fig.7. Commercial air-transducer inspection system.

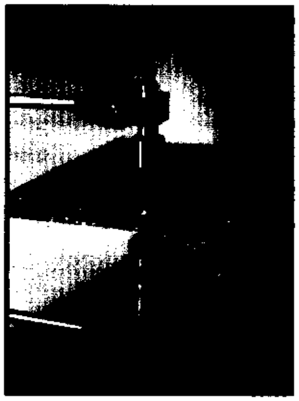

Fig. 8. C-scan inspection configuration with piezoelectric transducers

Past applications of the system include inspections of carbon-carbon composites for the presence of internal porosity, testing of foam-sandwich composites, evaluations of face-sheet bonding in solar-cell support panels, and similar applications. Typically, the system is operated either in a "through-transmission" mode, as shown in Fig. 8, or in a "pitch-catch" mode in which both transducers are located on the same side of the part undergoing inspection.

As shown in Fig. 9, the system typically operates in a tone-burst mode at the center frequency of 400 kHz, corresponding to an in-air wavelength of 0.85 mm, and uses spherically focused, piezoelectric elements with 50 mm nominal focal length and 25 mm diameter. However, it is also possible to operate the system at 200 kHz and 1 MHz, with small adjustments to accommodate transducer resonant-frequency variations. It is also possible to use other transducers. For example, the system can operate using conventional, piezoelectric contact and water-immersion transducers, and special transducers, such as "roller probes" and other "dry-contact" types.

To improve impedance-matching to the air, air transducers use a thin layer of a light polymeric-matrix, porous material with a specific impedance of approximately 1 Mrayl. The system, as shown in Figs. 7 and 9, utilizes a 500 V peak-to-peak bipolar driver with a very low output impedance, which is driven by a 15-cycle burst with 1-kHz pulse-repetition frequency, generated by an internal, computer-controlled tone-burst generator. Frequently, an impedance-matching network, not shown in Fig. 9, is used to increase the output of the transmitting transducer. The detected signals are first preamplified using a wide-band preamplifier circuit, with a 32-dB gain, which can be attached in-line with the receiver transducer. The preamplified signals are then scaled using a computer-controlled attenuator and filtered using a narrow-band, tunable amplifier with a 45-kHz bandwidth and amplified again using a variable-gain amplifier. At this point, the signals are digitized, using an 8-bit flash converter at a 10 Msample/s rate. Further processing is then accomplished by taking advantage of the internal, single-board computer, which also controls the display and permanent-recording functions. However, the peak-detection function is accomplished using a dedicated 8-bit comparator.

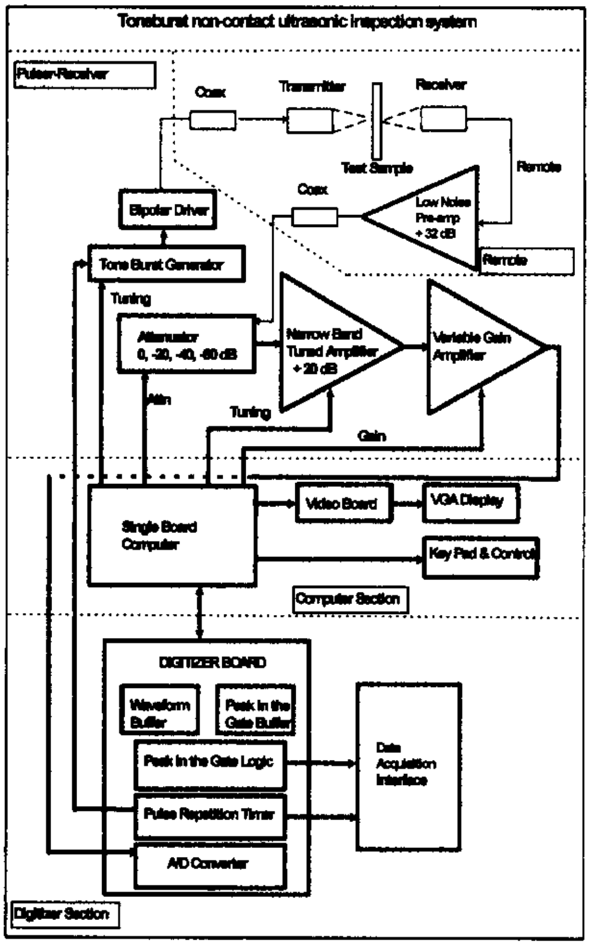

Fig. 9 Block diagram / system architecture of the inspection system of Fig. 7.

Figures 10 and 11 show C-scans of two materials used in aerospace applications: a fiber-reinforced epoxy panel and a honeycomb composite panel used to support solar cells.

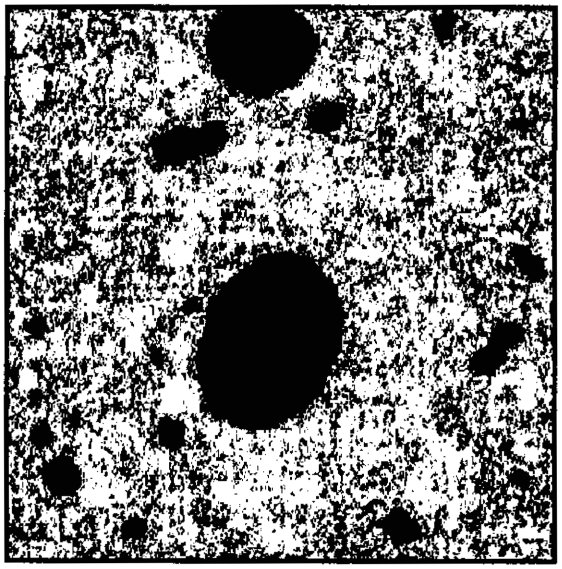

Fig. 10. C-scan image from an uncured phenolic/carbon fiber lay-up sheet. Panel size: 20 x 20 inch x 0.1 inch wall thickness. The dark areas outline the presence of delaminations. Measurements were taken with 400 kHz non-contact tone-burst method.

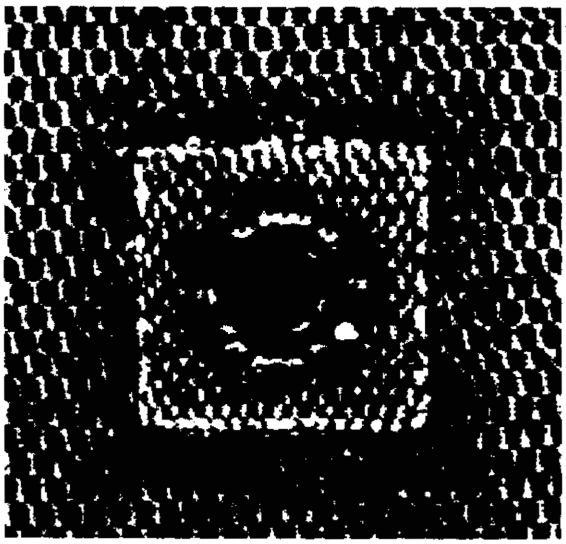

Fig. 11. C-scan image from a section of a solar honeycomb panel. This panel contains a reinforcement area which is inserted and bonded with foam adhesive into the surrounding honeycomb core structure. Note the missing core cells adjacent to the insert. Measurements were taken with 400 kHz non-contact toneburst method.

VI. A SYSTEM FOR DEMONSTRATING THE FEASIBILITY OF IN-LINE INSPECTION OF NATURAL-GAS PIPELINES

Ultrasonic inspection of large-diameter, natural-gas pipelines presents a great challenge to the gas-coupled transducer technology. Natural gas exhibits a very low specific acoustic impedance (300 Rayls for methane at atmospheric pressure) compared to oil (1.5 Mrayls and higher). Consequently, even at working pressures (6.9 MPa or 1000 psi), the ultrasonic-signal reflections from the pipe-wall/gas interfaces are significantly larger than the signals returned from the outer surface of the pipe wall. To circumvent this obstacle, past exploratory developments included the use of a liquid-filled wheel[70], electromagnetic-acoustic-transducer (EMAT)[71] , and liquid-slug technologies[72] . While prototypes of high-speed, in-line inspection systems employing such principles do exist, all exhibit serious operational shortcomings that prevent widespread commercial exploitation.

An alternative concept of an automated ultrasonic system for detecting thickness variations and crack-like flaws in the pipe wall is shown in Fig. 12. The concept shown in Fig. 12 would use the natural gas as an ultrasonic couplant and would be functionally similar to a liquid-coupled system, using similar electronics and transducers. As shown in Ref. 55, operation in the pulse-echo mode, which is very desirable but not currently possible at atmospheric pressures, can be achieved at pressures typical of pipelines.

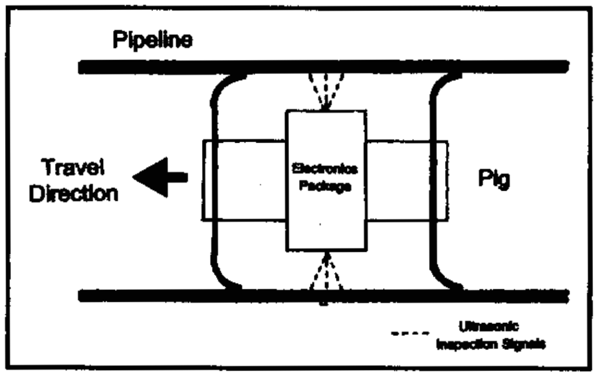

Fig. 12.Concept of an automated ultrasonic system for pipe wall inspection.

Figure 13 shows the functional block diagram of an experimental system developed at NIST to demonstrate the feasibility of the concept illustrated in Fig. 12. The experimental system uses a cylindrical pressure vessel, 305 mm (12 in) in diameter and 610 mm (24 in) in length. The pressure vessel can accommodate a variety of gases at pressures up to 10 MPa (1500 psi) and has appropriate feed-throughs for sample and transducer-motion control, signal handling, and pressure and temperature monitoring. Inside the vessel, a flexible stage with multiple degrees of freedom manipulates both the transducer and samples. Also, four position-adjustment motors are used to manipulate the Z coordinate of the sample and the X, Y, and θ coordinates of the pulse-echo transducer. The coordinate θ is the angle in the sagittal plane between the transducer symmetry axis and the normal to the plate-surface.

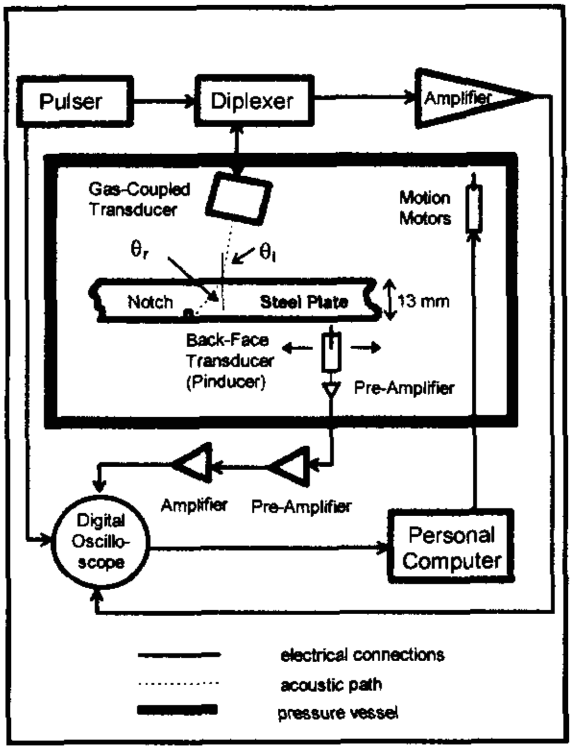

Fig. 13. Functional block diagram of experimental system for showing feasibility of inspecting gas pipelines.

The experimental system shown in Fig. 13 uses a flat, wide-band, piezoelectric-ceramic transducer, 13 mm (0.5 in) in diameter to generate and receive the ultrasonic signals. The transducer, which is constructed as shown in Fig. 5f, exhibits a center frequency of 2.25 MHz when operated in water. To generate, detect, and condition the ultrasonic signals, we use a square-wave pulser with 8 kW available peak power at 400 V, a special diplexer circuit, and a receiver amplifier of high-input impedance with 64 dB dynamic range and 60 MHz bandwidth. Manually stepped attenuators control the output-pulse power levels and receiver-amplifier gains. We also use an 8-bit digital storage oscilloscope (DSO) sampling at 400 MHz to record the signal waveforms. A dedicated computer controls the setup. As shown in Fig. 13, there is another transducer coupled directly to the back surface of the flat-plate specimen. Specifically, a pin transducer, 1.4 mm (0.06 in) in diameter provides ultrasonic-beam diagnostics and aid in initial alignment.

In Figure 13, the specimens are two surface-ground flat steel plates. Each is 114 mm (4.5 in) long, 44 mm (1.75 in) wide, and 13 mm (0.5 in) thick. The two plates are typically mounted side by side and contain thin, surface-breaking notches made by standard electro-discharge machining (EDM) procedures. The notch depths are 20% and 40% of the nominal plate thickness, *i.e.*, 2.5 mm (0.1 in) and 5.1 mm (0.2 in). The notches have mouth widths of 0.3 mm (0.01-in) and are 44 mm (1.75 in) long.

In principle, the experimental arrangement shown in Fig. 13 is useful for measuring the thickness of the plate, finding delaminations in the plane of the plate, and detecting vertical cracks. Wall thickness is best measured using longitudinal-wave signals that propagate along the plate-surface normal. Such signals result from compressional-wave signals in the gas that propagate along the plate-surface normal direction (θ_i = 0°). On the other hand, vertical cracks are best detected with longitudinal- or shear-wave signals that propagate at an angle (θ_r) with respect to the plate-surface normal. To generate such signals, the symmetry axis of the pulse-echo transducer must rotate in the sagittal plane to satisfy Snell's law for both longitudinal- and shear-wave signals.

Figure 14 shows an experimental configuration for detecting wall thickness variations. The ultrasonic signals are shown in Fig. 15. The first signal in Fig. 15 is due to the direct reflection off the front surface of the plate specimen (a). The following signals are multiple reverberations within the plate (b and c). Here, the transducer-plate separation distance is 38 mm (1.5 in) and the pressure (nitrogen) is 6.9 MPa (1000 psi). The time-domain separation between the ultrasonic reverberations in the flat plate (b and c) is approximately 4 μs, consistent with the nominal plate thickness of 12.7 mm (0.5 in).

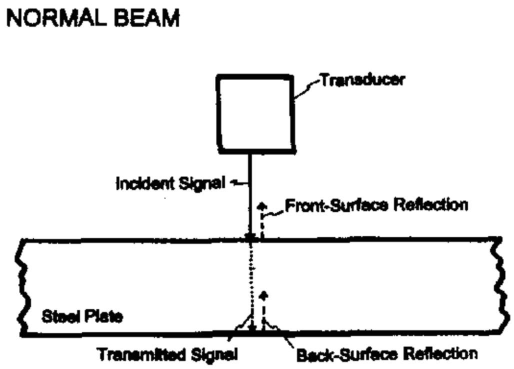

Fig. 14. Experimental configuration for detecting wall thickness variations

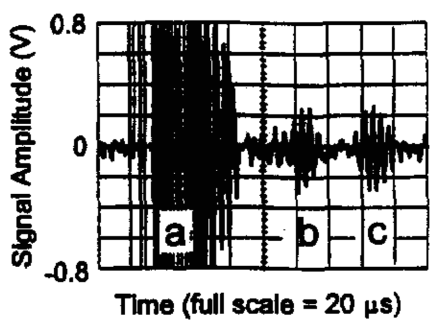

Fig. 15. Ultrasonic signal from the configuration of Fig. 14.

Figure 16 shows the experimental configuration for detecting internal crack-like flaws. In principle, both longitudinal- and shear-wave signals are useful in a pulse-echo configuration for detecting flaws. In water-coupled systems, longitudinal-wave signals are preferable. Although both longitudinal- and shear-wave flaw signals are observed experimentally, the latter clearly separate from the front-surface reflection signals. The A-scan in Fig. 17 illustrates this effect. The longitudinal-wave flaw signal occurs at only 6 μs after the first observable front-surface reflection. Although it is possible to detect the presence of the vertical notch (40% of wall thickness) by monitoring the behavior of the interferences between the two signals, the process is not reliable. On the other hand, the shear-wave reflections, arriving at approximately 11 μs following the beginning of the front-surface reflection, are clearly discernible.

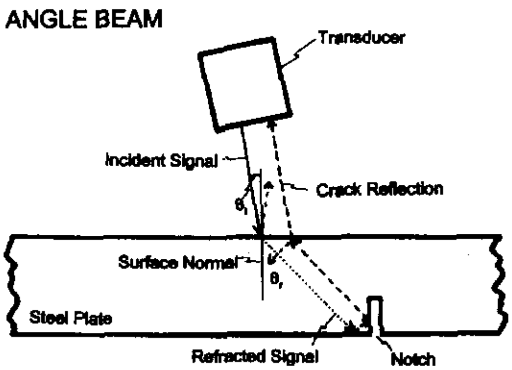

Fig.16. Experimental configuration for detecting internal, crack-like flaws

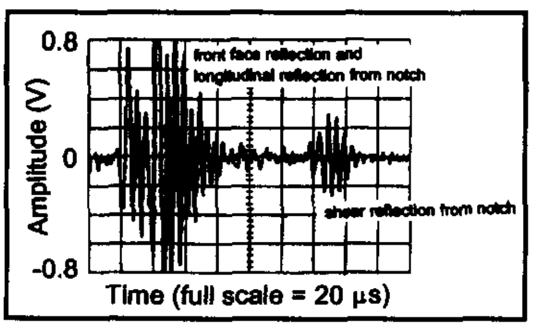

Fig. 17. A-scan of the experimental configuration of Fig. 16.

The above experimental results clearly demonstrate that it may be feasible to use pressurized natural gas as the ultrasonic couplant in a pulse-echo system to detect flaws and measure thickness in natural-gas pipelines. Because sound propagates much more slowly in a gas than in water, (300-500 m/s vs. 1500 m/s), the incidence angles of the ultrasonic probes are correspondingly smaller. Furthermore, sensitivity to misalignment is expected to be greater for gas-coupled systems than for liquid-coupled systems. Further developments in this area will be needed to show the practicality of the concept. In particular, additional studies will be needed to explore the impact of surface roughness, pipe-wall curvature, and gas composition and temperature.

VII. PULSE-ECHO ACOUSTIC MICROSCOPY

We have also used the system as shown in Fig. 13 with a spherically focused instead of a flat transducer. More detailed information on this system can be found in Ref. 51. Both, polymer-piezoelectric and piezoelectric-ceramic transducers, can be used, depending on the frequency of operation. The support electronics is essentially identical to that used in the experiment designed to demonstrate the feasibility of in-line inspection of natural-gas pipelines. Figure 18 shows a nominally 2.25-MHz, pulse-echo C-scan of a 25-cent coin embedded in a PMMA plate. Argon, at 30 atmospheres, is used as the coupling gas and the coin is located approximately 7.5 mm below the front surface of the PMMA plate. While the image shown in Fig. 18 demonstrates the feasibility of a gas-coupled microscope, much work remains to be done in order to show practicality of the concept. Potential applications may include the inspection of electronic chips mounted on ceramic substrates[73].

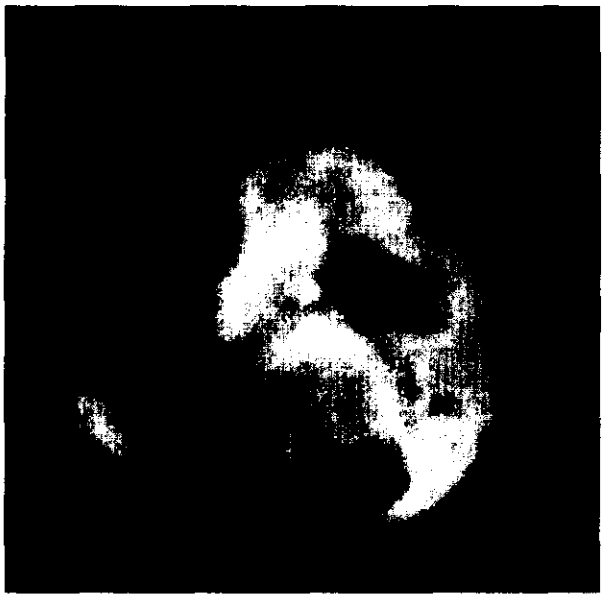

Fig. 18. C-scan of a 25-cent coin embedded in PMMA

VIII. FUTURE POSSIBILITIES

In light of the recent advances in air transducer technologies, it is interesting to compare the sensitivity limits of various ultrasonic transducers with ideal and micromachined air transducers. Figure 19, which is obtained from a companion paper[74], shows the calculated sensitivity limits, in terms of a time-averaged, minimum-detectable displacement, in a 1-Hz bandwidth, of optical interferometers, EMATs, direct-contact (piezoelectric), and capacitive air transducers. The absolute limit, as calculated using the fluctuation-dissipation theorem as assuming an ideal (loss-less and mass-less) transducer, is also shown.

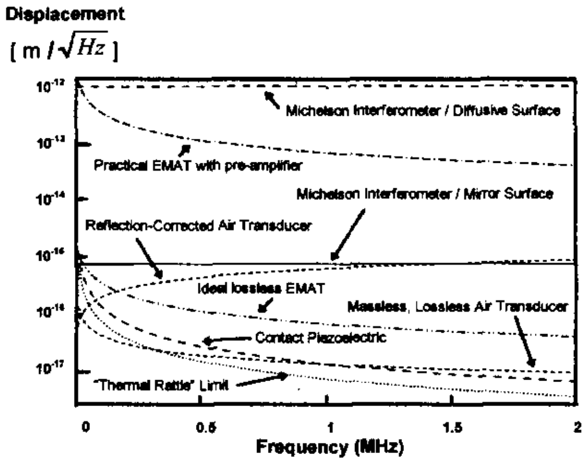

Fig. 19. Minimum detectable displacements

It is interesting to note that, in the 0.5-1.5 MHz frequency region, the absolute limit, as determined using a fluctuation-dissipation argument, is approximately $10^{-17}\text{m}/\sqrt{Hz}$. This limit can be readily approached using piezoelectric, contact transducers. However, all of the practical non-contact transducers are significantly less sensitive. In particular, a 100-mW laser interferometer can achieve only $10^{-15}\text{m}/\sqrt{Hz}$, while a practical EMAT can achieve only $10^{-14}\text{m}/\sqrt{Hz}$. On the other hand, an ideal air transducer, assuming perfect acoustic matching to the air, can achieve approximately $10^{-16}\text{m}/\sqrt{Hz}$. In the case of a piezoelectric transducer, which exhibits one-way losses of approximately 40 dB, the above limit would be $10^{-14}\text{m}/\sqrt{Hz}$. However, a much better performance can be expected of a capacitive transducer with a very thin membrane. In this case, the reduction in sensitivity can be estimated using the ratio of acoustic impedance of air and Eq. 4 to estimate the acoustic impedance of the membrane[75]. Thus, assuming a 1-μm silicon membrane, the reduction in sensitivity is approximately 32 at 1 MHz. Consequently, well-designed capacitive air transducers can be expected to be as sensitive as the best laser interferometers. As a result, such transducers can replace lasers as detectors in those applications where proximity of the receiver transducer to the specimen is not critical. Also, the new micromachined air transducers should be considered for use in conventional and developmental air-coupled ultrasonic NDE systems, such as those described in this paper.

X. SUMMARY

This paper reviews the state of the art in air-coupled transduction in the context of ultrasonic NDE applications. The paper mainly focuses on the recent developments in the United States and, consequently, complements the paper presented by D.A. Hutchins at the 1994 IEEE Ultrasonic Symposium in Cannes, France. In particular the paper describes the capabilities of a commercially available air-coupled system and potential new applications, such as pulse-echo, in-line inspection of natural-gas pipelines and acoustic microscopy. Also, an argument is made for exploring the use of the newly developed micromachined capacitive transducers as a viable alternative to the currently used piezoelectric and previous-generation capacitive air transducers.

X. ACKNOWLEDGMENT

The authors are indebted to many individuals who have contributed their talents to the system developments described in this paper. In particular, the authors would like to acknowledge R.E. Schramm, J.D. McColskey, and M.C. Renken at NIST, C.M. Teller, Al Crouch, and Jerry Jackson at the Southwest Research Institute. The authors also thank B.T. Khuri-Yakub, P. Cawley, G.A. Hayward, D.W. Schindel, and D.A. Hutchins, and M.A. Anderson for very helpful comments and references to past and current work.Thanks to Jan Strycek for all his support in the development work, related to the practical non-contact ultrasonic instrumentation. Also thanks to H.P Loertscher and Karin Blinn-Grandia for their suggestions and editing contributions.

XI. DISCLAIMER

Mention of a particular commercially available system, component, or material (for scientific completeness) does not constitute endorsement by the National Institute of Standards and Technology.

[1] J. Krautkraemer and H. Krautkraemer, "Ultrasonic Testing of Materials, 4th Fully Revised Edition" (Springer-Verlag, Berlin, 1989).
[2] R.B. Thompson, "Noncontact Transducers", in Proc. 1977 Ultrasonics Symp., B.R. McAvoy ed. (IEEE, New York, 1977) pp. 74-83.
[3] D.A. Hutchins and D.W. Schindel, "Advances in Non-Contact and Air-Coupled Transducers", in Proc. 1994 Ultrasonics Symp., B.R. McAvoy ed. (IEEE, New York, 1994) pp. 1245-1254.
[4] B.W. Maxfield and C.M. Fortunko, "The Design and Use of Electromagnetic Acoustic Transducers (EMATs)", Mat. Eval. 41(12), Dec. 1983, pp. 1399-1408.
[5] G.A. Alers and L.R. Burns, "EMAT Designs for Special Applications", Mat. Eval. (45), Oct. 1987, pp. 1184-1189.
[6] R.B. Thompson, "Physical Principles of Measurements with EMAT Transducers", in Phys. Acoustics, R.N. Thurston and A.D. Pierce eds. (Academic Press, New York, 1990) pp. 157-200.
[7] B.W. Maxfield, A. Kuramoto, and J.K. Hulbert, "Evaluating EMAT Designs for Selected Applications", Mat. Eval. Vol. 45, Oct. 1987, pp. 1166-1183.
[8] C.B. Scruby and L.E. Drain, "Laser Ultrasonics" (Adam Hilger, Bristol, 1990)
[9] P. Cielo, "Optical Techniques for Industrial Inspection" (Academic Press, New York, 1988)
[10] J. Wagner, "Optical Detection of Ultrasound", in Physical Acoustics, R.N. Thurston and A.D. Pierce eds. (Academic Press, New York, 1990) pp. 201-266.
[11] A.V. Clark, S.R. Schaps, and C.M. Fortunko, "A Well-Shielded EMAT for On-Line Ultrasonic Monitoring of GMA Welding", in Proc. 1991 Ultrasonics Symp., B.R. McAvoy ed. (IEEE, New York, 1991) pp. 337-340.
[12] N.M. Carlson, J.A. Johnson, and J.G. Rodriquez, "Enhancement of Laser/EMAT Ultrasonics", in Proc. 1994 Rev. Prog. in QNDE, Vol.

13, D.O. Thompson and D.E. Chimenti eds. (Plenum, New York, 1994) pp. 709-715.
[13] D.A. Hutchins, D.P. Jansen, and C. Edwards, "Lamb-Wave Tomography Using Non-Contact Transduction", Ultrasonics 31(2), 1993, pp. 97-103.
[14] D.A. Hutchins, W.M.D. Wright, G. Hayward, and A. Gachagan, ""Air-Coupled Piezoelectric Detection of Laser-Generated Ultrasound", IEEE Trans. UFFC, Vol. 41(6), 1994, pp. 796-805.
[15] A.J. Rogovsky, "Development and Application of Air-Coupled Ultrasonic Dry-Contact and Air-Coupled C-Scan Systems for Nondestructive Evaluation of Aerospace Composites", Mat. Eval. 50(12), Dec. 1991, pp. 1401-1497.
[16] M.J. Anderson, P.R. Martin, and C.M. Fortunko, "Gas-Coupled Ultrasonic Measurement of Stiffness Moduli in Polymer Composite Plates", in Proc. 1994 Ultrasonics Symp., B.R. McAvoy ed. (IEEE, New York, 1994) pp. 1255-1260.
[17] P.R. Martin, "Determination of the Elastic Constants of Composites Using Air Coupled Ultrasonic Data", M.S. Thesis, University of Idaho, Moscow, ID, 1995.
[18] A. Safaeinili, O.I. Lobkis, and D.E. Chimenti, "A Robust Technique for Estimating Visco-Elastic Constants of Plates", these Proceedings.
[19] M.J. Anderson, P.R. Martin, and C.M. Fortunko, "Resonance Transmission of a 3 Dimensional Sound Beam Through a solid Plate in Air; Theory and Measurements", JASA, in press.
[20] D.A. Hutchins, W.M.D. Wright, and D.W. Schindel, "Ultrasonic Measurements in Polymeric Materials Using Air-Coupled Capacitance Transducers", J. Acoust. Soc. Am. 96(3) Sept. 1994, pp. 1634-1642.
[21] M. Castaings and P. Cawley, "Air-Coupled Ultrasonic Transducers for the Detection of Defects in Plates", in Proc. 1995 Rev. Prog. in QNDE, Vol. 15, D.O. Thompson and D.E. Chimenti eds. (Plenum, New York, 1995) in press.
[22] R. Farlow, S. Kelly, G. Hayward, "Advances in Air-Coupled NDE for Rapid Scanning Applications", in Proc. 1994 Ultasonics Symp., B.R. McAvoy ed. (IEEE, New York, 1994) pp. 1099-1102.
[23] D.A. Hutchins, W.M.D. Wright, G. Hayward, and A. Gachagan, "Evaluation of Fiber-Reinforced Composites Using a Non-Contact Laser/Air-Transducer System", 1994 Rev. Prog. QNDE, D.O. Thompson and D.E. Chimenti eds. (Plenum, New York, 1994) pp. 1333-1340.
[24] W. Johnson, B.A. Auld, and G.A. Alers, "Spectroscopy of Resonant Torsional Modes in Cylindrical Rods Using Electromagnetic-Acoustic Transduction", J. Acoust. Soc. Am. 95(3), March 1994, pp. 1413-1418.
[25] D.S. Dean, "Towards an Air Sonar", Ultrasonics, Jan. 1968, pp. 29-38.
[26] V. Magori, "Ultrasonic Sensors in Air", in Proc. 1994 Ultrasonics Symp., B.R. McAvoy ed. (IEEE, New York, 1994) pp. 471-481.
[27] L.C. Lynnworth, "Ultrasonic Impedance Matching from Solids to Gases", IEEE Trans. Sonics and Ultrasonics, SU-12(2), June 1965, pp. 37-48.
[28] L.C. Lynnworth, "Ultrasonic Measurements for Process Control" (Academic Press, New York, 1989)
[29] F. Massa, "An Efficient Low-Cost Ultrasonic Transducer for Use in Remote Control and Carrier Frequency Applications", IRE National Conv. Rec. 8(6), 1960, pp. 243-245.
[30] F. Massa, "Ultrasonic Transducers for Use in Air", IEEE Proc. 53(10) Oct. 1965, pp. 1363-1371.
[31] W. Kuhl, G.R. Schrodder, and F.-K. Schroeder, "Condenser Transmitters and Microphones with Solid Dielectric for Airborne Transducers" Acustica 4(5), Apr. 1954, pp. 519-532.
[32] W.W. Wright, Technical Memorandum No. 47, Acoustics Research Laboratory, Harvard Univ., Apr. 1962.
[33] W.W. Wright, "High Frequency Electrostatic Transducers for Use in Air", IRE National Conv. Rec. 10(6), 1962, pp. 95-100.
[34] C. Biber, S. Ellin, E. Shenk, and J. Stempeck, "The Polaroid Ultrasonic Ranging System", presented at the 67th Convention of the Audio Engineering Society, Oct. 31-Nov. 3, 1980.
[35] B.T. Khuri-Yakub, J.H. Kim, C-H. Chou, P. Parent, and G.S. Kino, "A New Design for Air Transducers", in Proc. 1988 Ultrasonics Symp., B.R. McAvoy ed. (IEEE, New York, 1988) pp. 503-506.
[36] M.R. Moldover, J.P.M. Trusler, and T.J. Edwards, J.B. Mehl and R.S. Davis, "Measurement of the Universal Gas Constant R Using a Spherical Resonator", J. Res. NBS 93(2), March 1988, pp. 85-140.
[37] Martin Greenspan, "Propagation of Sound in Five Monatomic Gases", JASA 28(4), July 195, pp. 644-648.
[38] J.P.M. Trusler, "Physical Acoustic and Metrology of Fluids" (Adam Hilger, Bristol, 1991) pp. 116-178.
[39] R. Hickling and S.P. Marin, "The use of ultrasonics for gauging and proximity sensing in air", JASA 79(4), April 1986, pp. 1151-1159.
[40] H.E. Bass, L.C. Sunderland, Joe Percy, and Landon Evans, "Absorption of Sound in the Atmosphere", in Phys. Acoust. Vol. XVII, W.P. Mason ed. (Academic Press, New York, 1984) pp. 145-232.
[41] E.H. Brown and S.F. Clifford, "On the Attenuation of Sound by Turbulence", JASA 60(4), 1976, pp. 788-794.
[42] H.J. Bass, L.C. Sutherland, and A.J. Zuckerwar, "Atmospheric Absorption of Sound: Update," JASA 88(8), 1990, pp. 2019-2021.
[43] H.E. Bass, L.C. Sutherland, and A.J. Zuckerwar, "Atmospheric Absorption of Sound: Further Developments", JASA 97(1) 1995, pp. 680-683.
[44] L.J. Bond, C-H. Chiang, and C.M. Fortunko, "Absorption of Ultrasonic Waves in Air at High Frequencies (10-20 MHz)", JASA 92(4), 1992, pp. 2006-2015.
[45] J. Szilard, "Ultrasonic Testing, Non-conventional Testing Techniques" (Wiley, New York, 1982) pp. 400-402.
[46] D.S. Dean, Rocket Propulsion Establishment, Westcott, Technical Report No. 65/10, 1965.
[47] A.S. Birks, "Particleboard Blow Detector", Forest Products J. 22(6), June 1972, pp. 23-26.
[48] M. Luukkala, P. Heikkila, and J. Surakka, "Plate Wave Resonance-a Contactless Testing Method", Ultrasonics 9, Oct. 1971, pp. 201-208.
[49] A. Murray, "Air-Coupled Ultrasound Used to Detect Flaws in Paintings on Wooden Panels", Ph.D. thesis, The Johns Hopkins University, Baltimore, MD, 1993.
[50] D.E. Chimenti and C.M. Fortunko, "Characterization of Composite Prepreg with Gas-Coupled Ultrasonics", Ultrasonics 32(4), 1994, pp. 261-264.
[51] M. Luukkala, "Tenscan, an Acoustic NDE Device to Measure Tension in a Moving Paper Web", in 1990 Rev. Prog. in QNDE, D.O. Thompson and D.E. Chimenti eds. (Plenum, New York, 1990) pp. 1987-1981.
[52] V.I. Zaklyukovskii and G.T. Kartsev, "Use of Piezoelectric Transducers for Contactless Ultrasonic Product Inspection", Defektoskopiya (Sov. J. NDT) 3, Mar. 1978, pp. 28-34.
[53] W.A. Grandia, "Advances in Nondestructive Testing - Noncontact Ultrasonic Inspection of Composites", in Proc. 39th International SAMPE Symp., Vol. 39, Book 1, K. Drake, J.Bauer, T. Serafini, and P.Cheng eds., 1994, pp. 1308-1315.
[54] M. Deka, "Air-coupled Ultrasonic Transducer for NDE", in 1987 Ultrasonics Symp. Proc., B.R. McAvoy ed. (IEEE, New York, 1987) pp. 543-546.
[55] C.M. Fortunko, R.E. Schramm, C.M. Teller, G.M. Light, J.D. McColskey, W.P. Dube, and M.C. Renken, "Gas-Coupled, Pulse-Echo Ultrasonic Crack Detection and Thickness Gaging", in Proc. 1994 Review of Progress in Quantitative NDE, edited by D.O. Thompson and D.E. Chimenti (Plenum Press, New York, 1995), pp. 951-958.
[56] C.M. Fortunko, W.P. Dube, and J.D. McColskey' "Gas-Coupled Acoustic Microscopy in the Pulse-Echo Mode", in Proc. 1993 Ultrasonics Symp., B.R. McAvoy ed. (IEEE, New York, 1993) pp. 617-618.

[57] H.K. Wickramasinghe and C.R. Petts. "Acoustic Microscopy in High-Pressure Gases", in Proc. 1980 Ultrasonics Symp., B.R. McAvoy ed. (IEEE, New York, 1980) pp. 668-670.
[58] -, American National Standard, Method for the Calculation of the Absorption of Sound by the Atmosphere, ANSI S1.26-1978, (American Institute of Physics, New York, 1978)
[59] N.I. Prudko, PiezotecniX, Dniepropetrovsk, the Ukraine, private communication.
[60] B.T. Khuri-Yakub, Stanford University, private communication.
[61] M.I. Haller and B.R. Khuri-Yakub, "1-3 Composites for Ultrasonic Air Transducers", in Proc. 1992 Ultrasonics Symp., B.R. McAvoy ed. (IEEE, New York, 1992) pp. 937-939.
[62] W.A. Smith, "The Role of Piezocomposites in Ultrasonic Transducers", in Proc. 1989 Ultrasonics Symp., B.R. McAvoy (IEEE, New York, 1989) pp. 755-766.
[63] (-), "Condenser Microphones and Microphone Preamplifiers for Acoustic Measurements; Data Handbook" (Bruel & Kjaer, Naerum, 1982)
[64] G.S.K. Wong and T.F.W. Embleton, "AIP Handbook of Condenser Microphones; Theory, Calibration, and Measurements" (American Institute of Physics, New York, 1995)
[65] H. Carr and C. Wykes, "Diagnostic Measurements in Capacitance Transducers", Ultrasonics 31(1) 1993, pp. 13-20.
[66] P. Mattila, f. Tsuzuki, H. Vaataja, K. Sasaki, "Electroacoustic Model for Electrostatic Ultrasonic Transducers with V-Grooved Back Plates", IEEE Trans. Ultrasonics, Ferroelectrics, and Freq. Control" 42(1), 1995, pp. 1-7.
[67] M.J. Anderson, J.A. Hill, C.M. Fortunko, N.S. Dogan, and R.D. Moore, "Broadband Electrostatic Transducers; Modeling and Experiments", J. Acoust. Soc. Am. 97(1), 1995, pp. 262-272.
[68] D.W. Schindel, D.A. Hutchins, Linchun Zou, and M. Sayer, "The Design and Characterization of Micromachined Air-Coupled Capacitance Transducers", IEEE Trans. Ultrasonics, Ferroelectrics, and Frequency Control 42(1), Jan. 1995, pp. 42-50.
[69] M.I. Haller, "Micromachined Ultrasonic Devices and Materials", Ph.D. Thesis, Stanford University, 1994.
[70] C.R. Ward and A.S. Mann, in 8th Symp. on Pipeline Research, Houston, TX, Sept. 26-29, 1993, paper 21.
[71] G.A. Alers and L.R. Burns, ibid.
[72] J.A. de Raad and J.v.d. Ent, in Proc. 12th World Conf. on Non-Destruct. Test., eds. J. Boogaard and G.M. van Dijk (Elsevier, Amsterdam, 1989) p. 667.
[73] L.W. Kessler, Sonoscan, Inc., private communication.
[74] E.S. Boltz and C.M. Fortunko, "Absolute Sensitivity Limits of Various Transducers", in these Proceedings.
[75] J.H. Cantrell and W.T. Yost, "Liquid-Membrane Coupling Response of Submersible Electrostatic Acoustic Transducer", Rev. Sci. Instrum. 60(3), Mar. 1989, pp. 487-488.